PMSM Model with Phase-to-Phase Short-Circuit and Diagnosis by ESA and EPVA

Chourouk BOUCHAREB, Mohamed Said NAIT SAID

Electrical Engineering Department, Laboratory LSPIE Batna 2000, Batna University, Route de Biskra, 05078, Algeria

c.bouchareb@live.fr, medsnaitsaid@yahoo.fr

DOI: 10.15598/aeee.v14i5.1928

Abstract. *One of the most frequent faults in PMSM stator is the insulation failure due to the degradation of the main isolation in the motor winding. This paper is aimed at suggesting a dynamic model of PMSM with phase-to-phase fault based on an equivalent electric circuit model including the real form of back EMF. The faulty model is used for studying the machine behavior and extracting the fault signatures for diagnosis. Two diagnostic techniques the Spectral Analysis (ESA) and Extend Park's Vectors Approach (EPVA) based on frequency analysis are applied to detect this kind of fault.*

Keywords

EPVA, ESA, Inter-turn fault, phase-to-phase fault, PMSM model.

1. Introduction

In recent years, Permanent Magnet Synchronous Motor (PMSM) has become one of most important electric machines because of the inherent advantages of high power density, high efficiency, small weight, high reliability and easy control of external torque of stator's current control. Consequently, it is widely used in industry, e.g. in traction, automobiles, robotics and aerospace technology, as well as electric vehicles and ship propulsion systems [1], [2] and [3].

The fault diagnosis of electrical machines had been the target of an intense amount of interesting researches during the last 30 years. Reducing maintenance costs and preventing unscheduled down-times, which result in losses of production and financial incomes and benefitting from their utility in safety-sensitive applications, are the priorities of electrical drives for manufacturers and operators [4], [5] and [6].

In fact, correct diagnosis and early detection of incipient faults require the development of an accurate model for electrical machine, able to simulate electrical faults and to apply an effective diagnostic technique.

However, model accuracy and computation time represents two opposite criteria. Conventional model (equivalent electric circuit or equivalent magnetic circuit) obtained with Park transformation for instance is based on restrictive assumptions and does not require long computation time [7] and [8]. On the other hand, model obtained with the finite elements method is based on minimal assumption and requires long computation time [9] and [10]. There is a real need to establish an alternative model, which offers a good balance between accuracy and computation time.

One of the most common faults, called insulation failure, is the inter-turn short circuit in one of the stator coils. Since the coil insulation material is under the high voltage and temperature stress, it degrades gradually and finally loses the insulating characteristic [6]. The inter-turn fault is mostly caused by mechanical stress, moisture and partial discharge, which is accelerated for inverter supplied electrical machines [11].

In this paper, a dynamic model of a stator surface mounted PMSM with inter-turn fault is presented. We focus on phase-to-phase fault of the stator winding. This model based on equivalent electric circuit exhibits a trade-off between simplicity and precision, and it is used for studying a machine behavior under fault conditions for different levels of fault severity using MATLAB Simulink software.

Exploiting this faulty model to extract fault signatures in order to diagnose and to predict the insulation failure breakdown when the fault is not very severe in order to avoid the machine winding damages. To detect this fault, we chose two simple and useful techniques based on frequency analysis. These techniques are Electric Spectral Analysis (ESA) and Extend Park's Vectors Approach (EPVA). The contribution of this work is the addition of the real waveform of back Electro Motive Force (EMF) of healthy machine which contains a harmonic at $3 \cdot f_s$ of supply frequencies, because if the model does not take the uncertainties, like real back-EMF, the indicator will give a wrong diagnostic.

2. PMSM Fault Dynamic Model

2.1. Phase-to-Phase Fault Dynamic Model

The phase-to-phase fault denotes insulation failures between two windings of two phases at the stator. The insulation failure is modeled by a resistance, where its value depends on the fault severity. The stator winding of a PMSM machine with phase-to-phase fault is represented by Fig. 1. In this figure, the fault occurs between 'a' and 'b' phases, r_f denotes the fault insulation resistance. The sub-windings (a_{s1}) and (a_{s2}) represent respectively, the healthy and faulty part of the phase winding a, and sub-windings (b_{s1}) and (b_{s2}) represent, the healthy and faulty part of the phase winding b respectively. When the fault resistance r_f decreases towards zero, the insulation fault evaluates towards an inter-turn full short-circuit.

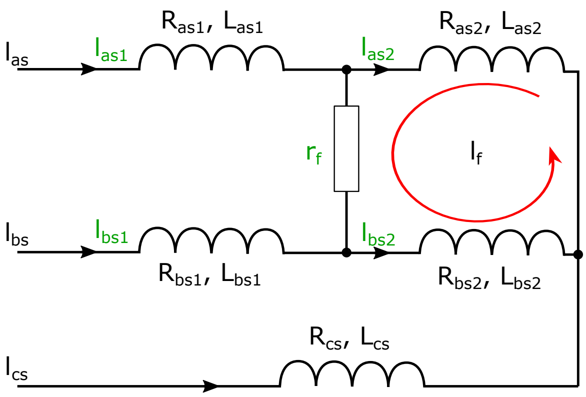

Fig. 1: Three-phases winding with phase-to-phase fault.

2.2. PMSM Healthy Model in abc-Coordinates

The voltages equations from the circuit in Fig. 1 without fault(healthy machine), given by r_f infinite value, as in [2], [12] and [13] are:

$$[V_s] = [R_s] \cdot [I_s] + [L_s] \cdot \frac{d}{dt} \cdot [I_s] + [E_s], \qquad (1)$$

$$\begin{bmatrix} v_{as} \\ v_{bs} \\ v_{cs} \end{bmatrix} = \begin{bmatrix} R_s & 0 & 0 \\ 0 & R_s & 0 \\ 0 & 0 & R_s \end{bmatrix} \begin{bmatrix} I_{as} \\ I_{bs} \\ I_{cs} \end{bmatrix} + \\ + \begin{bmatrix} L & M & M \\ M & L & M \\ M & M & L \end{bmatrix} \cdot \frac{d}{dt} \cdot \begin{bmatrix} I_{as} \\ I_{bs} \\ I_{cs} \end{bmatrix} + \begin{bmatrix} e_{as} \\ e_{bs} \\ e_{cs} \end{bmatrix}, \qquad (2)$$

where the healthy machine variable and parameters are:

- $v_{as,bs,cs}$ - three phase stator voltages,
- $I_{as,bs,cs}$ - three phase stator currents,
- $e_{as,bs,cs}$ - three phase back EMF,
- R_s - stator resistance,
- L - self inductance of the stator,
- M - mutual inductance of the stator.

2.3. PMSM Faulty Model in abc-Coordinate

Voltage equations, which describe the faulty circuit presented in Fig. 1, can be expressed as:

$$[V_s] = \begin{bmatrix} v_{as1} & v_{as2} & v_{bs1} & v_{bs2} & v_{cs} \end{bmatrix}^T, \qquad (3)$$

where:

- v_{as1} - the voltage of the healthy part phase a,
- v_{as2} - the voltage of faulty part of phase a,
- v_{bs1} - the voltage of the healthy part phase b,
- v_{bs2} - the voltage of faulty part of phase b.

The new resistances of healthy and faulty parts of phase 'a' and 'b' are calculated as follows:

$$R_{as1} = (1 - \sigma) \cdot R_{as}, \qquad (4)$$

$$R_{as2} = \sigma \cdot R_{as}, \qquad (5)$$

$$R_{bs1} = (1 - \sigma) \cdot R_{bs}, \qquad (6)$$

$$R_{bs2} = \sigma \cdot R_{bs}, \qquad (7)$$

$$\sigma = \frac{N_f}{N_s}. \qquad (8)$$

The study of the elementary circuits of the phases has given the following relations:

$$v_{as} = v_{as2} + v_{as1}, \qquad (9)$$

$$v_{bs} = v_{bs2} + v_{bs1}, \qquad (10)$$

$$I_{as1} = I_{as}, \tag{11}$$

$$I_{bs1} = I_{bs}, \tag{12}$$

where R_{as1} is the stator phase resistance of healthy parts of 'a' phase while R_{as2} is the faulty stator phase resistance. R_{bs1} it is the stator phase resistance of healthy parts of 'b' phase while R_{bs2} is its faulty stator phase resistance, σ is the ratioof number of the turns (N_f) over the phase winding number of the turns (N_s).

The self-inductances of the faulty and healthy parts of winding (a_{as1}, a_{as2}), and winding (b_{bs1}, b_{bs2}) are proportional to the square of the fraction of shorted turns σ, and also the mutual inductance is proportional to this number of both parts. Therefore, we assume:

$$L_{as1} = (1-\sigma)^2 L_{as}, \tag{13}$$

$$L_{as2} = \sigma^2 L_{as}, \tag{14}$$

$$M_{as2b} = \sigma M, \tag{15}$$

$$M_{as1as2} = \sigma (1-\sigma) L, \tag{16}$$

where L_{as1} is the stator phase inductance of healthy parts of a phase while L_{as2} is the stator phase inductance of faulty parts of a phase, I_f is the additional current engendered by the short circuit, r_f is the insulation faulty resistance and v_f is the corresponded faulty voltage.

The stator currents become:

$$[I_s] = [I_{as}\,(I_{as}-I_f)\,I_{bs}\,(I_{bs}+I_f)\,I_{cs}]^T. \tag{17}$$

The equation which describes the short circuit loop is in Eq. (18).

From previous analysis, we obtain the global equations governing the behavior of the machine with the presence of this short-circuit fault as the Eq. (19).

In the Eq. (19):

$$R' = R_{as} + R_{bs} + R_{cs}, \tag{20}$$

$$L_f = -\left(-L_{a2} + M_{a2b2} - L_{b2} + M_{b2a2}\right), \tag{21}$$

$$M_{bf} = -M_{a1a2} + M_{a1b2} - L_{a2} + M_{a2b2}, \tag{22}$$

$$M_{cf} = -M_{ca2} + M_{cb2}. \tag{23}$$

The expression of the electromagnetic torque can be written as follows:

$$T_e = \frac{e_{as}\cdot I_{as} + e_{bs}\cdot I_{bs} + e_{cs}\cdot I_{cs} - e_f \cdot I_f}{\Omega}, \tag{24}$$

where Ω is the mechanical angular speed.

2.4. PMSM Faulty Model in α,β-Coordinates

The machine equations with inter-turn fault in stationary α and β axis reference frame are in Eq. (25), where:

$$R_r = \sqrt{\frac{2}{3}}\left(-R_{a2} - \frac{R_{b2}}{2}\right), \tag{26}$$

$$r_f = R_{a2} + R_{b2} + R_f, \tag{27}$$

$$r_{b2} = \frac{1}{2}\sqrt{2}R_{b2}, \tag{28}$$

$$M_{f\alpha} = \sqrt{\frac{2}{3}}\left(M_{af} - \frac{M_{bf}}{2} - \frac{M_{cf}}{2}\right), \tag{29}$$

$$M_{f\beta} = \frac{1}{2}\sqrt{2}\left(M_{bf} - M_{cf}\right), \tag{30}$$

$$L_s = L - M, \tag{31}$$

with,

- $I_{\alpha,\beta}$ - α and β axis components of stator currents,
- $e_{\alpha,\beta}$ - α and β components of stator back EMF.

Then the electromagnetic torque expression for the phase-to-phase fault model becomes:

$$T_e = \frac{e_\alpha \cdot I_\alpha + e_\beta \cdot I_\beta - e_f \cdot I_f}{\Omega}. \tag{32}$$

We consider for all the studies that the electromotive force of the healthy motor has a sinusoidal form as shown in Fig. 2(a) and contains a 3rd harmonic at $3\cdot f_s$ of supply frequencies as seen in Fig. 2(b).

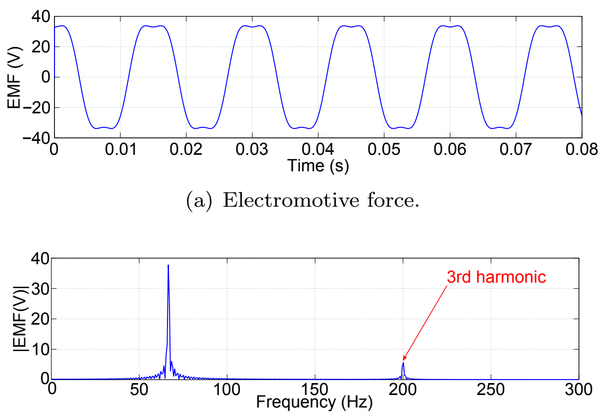

(a) Electromotive force.

(b) Spectrum analysis.

Fig. 2: Electromotive force and its spectrum analysis.

$$0 = -R_{a2} \cdot I_{as} + R_{b2} \cdot I_{bs} - (L_{a2} + M_{a1a2} - M_{b2a1} - M_{b2a2}) \cdot \frac{dI_{as}}{dt} - (M_{a2b1} + M_{a2b2} - L_{b2} - M_{b2b1}) \cdot \frac{dI_{bs}}{dt} + \\ -(M_{a2c} - M_{b2c}) \cdot \frac{dI_{cs}}{dt} - e_f + (R_{a2} + R_{b2} + r_f) \cdot I_f - (-L_{a2} + M_{a2b2} - L_{b2} + M_{b2a2}) \cdot \frac{dI_f}{dt} \quad . \tag{18}$$

$$\begin{bmatrix} v_{as} \\ v_{bs} \\ v_{cs} \\ 0 \end{bmatrix} = \begin{bmatrix} R_s & 0 & 0 & R_{a2} \\ 0 & R_s & 0 & R_{b2} \\ 0 & 0 & R_s & 0 \\ -R_{a2} & R_{b2} & 0 & R' \end{bmatrix} \begin{bmatrix} I_{as} \\ I_{bs} \\ I_{cs} \\ I_f \end{bmatrix} + \begin{bmatrix} L & M & M & M_{af} \\ M & L & M & M_{bf} \\ M & M & L & M_{cf} \\ M_{af} & M_{bf} & M_{cf} & L_f \end{bmatrix} \frac{d}{dt} \begin{bmatrix} I_{as} \\ I_{bs} \\ I_{cs} \\ I_f \end{bmatrix} + \begin{bmatrix} e_{as} \\ e_{bs} \\ e_{cs} \\ -e_f \end{bmatrix} . \tag{19}$$

3. Dynamic Fault Model Simulation Results

The study of the behavior of PMSM under fault conditions using the proposed fault dynamic model requires an accurate knowledge of circuit parameters. The PMSM parameters are given as shown in AppA [2].

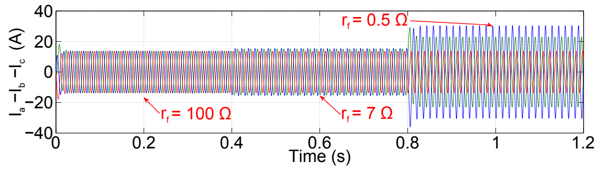

(a) Phase currents.

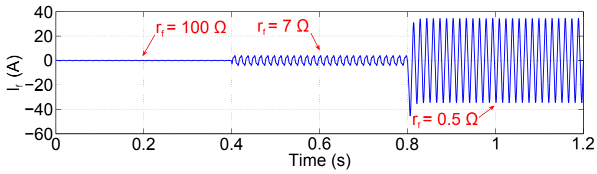

(b) Faulty current.

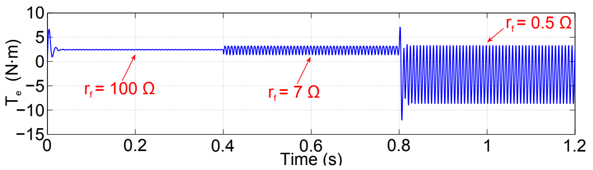

(c) Electromagnetic torque.

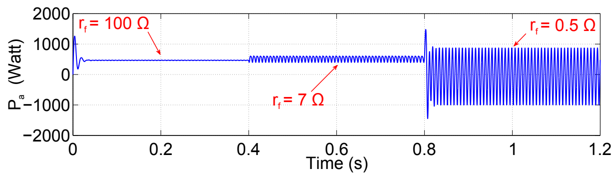

(d) Absorbed power.

Fig. 3: Phase currents, faulty current, electromagnetic torque and absorbed power versus time for three values of fault resistances: $r_f = 100\ \Omega$, $r_f = 7\ \Omega$ and $r_f = 0.5\ \Omega$.

The machine is supposed to be supplied by 3-phases sinusoidal balanced voltage source with star connection and without neutral connection and operates at synchronous speed (speed and supply frequency are 1000 rpm and 66.67 Hz respectively). Simulation of the proposed model is realized using MATLAB environment.

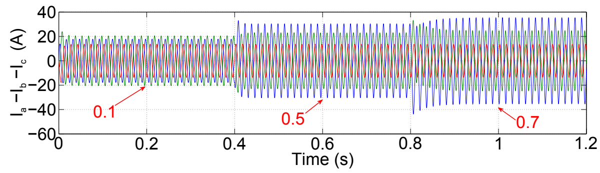

(a) Phase currents.

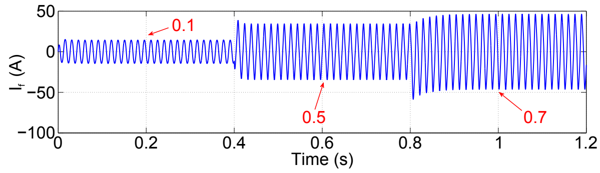

(b) Faulty current.

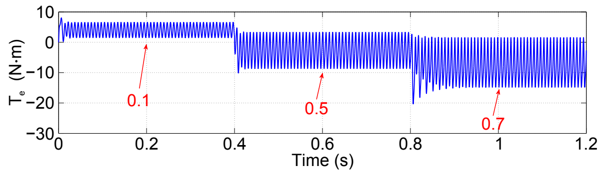

(c) Electromagnetic torque.

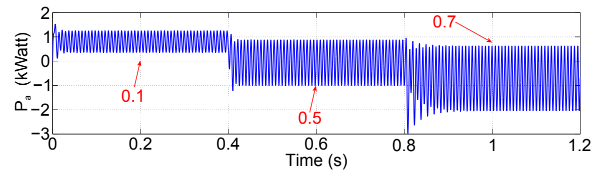

(d) Absorbed power.

Fig. 4: Phase currents, faulty current, electromagnetic torque and absorbed power versus time at three values of the fraction of shorted turns: ($\sigma = 0.1$, $\sigma = 0.5$ and $\sigma = 0.7$) and $r_f = 0.5\ \Omega$.

For this model, Fig. 3 shows the characteristics phase currents (a, b, c), faulty current (I_f), electromagnetic torque and absorbed power for different values of fault insulation resistance such as $r_f = 100\ \Omega$, 0.5 Ω and 7 Ω. The fraction of shorted turns is fixed at 50 %.

Figure 4 shows the characteristics (phase currents (a, b, c), faulty current (I_f), electromagnetic torque and absorbed power for different values of the fraction of shorted turns ($\sigma = 10\ \%$, $\sigma = 50\ \%$ and $\sigma = 70\ \%$), where the fault insulation resistance is fixed to $r_f = 0.5\ \Omega$.

As it can be seen from Fig. 3, for three different values of fault resistances (healthy case: $r_f = 100\ \Omega$ and

$$\begin{bmatrix} v_\alpha \\ v_\beta \\ 0 \end{bmatrix} = \begin{bmatrix} R_s & 0 & R_r \\ 0 & R_s & r_{b2} \\ R_r & r_{b2} & r_f \end{bmatrix} \cdot \begin{bmatrix} I_\alpha \\ I_\beta \\ I_f \end{bmatrix} + \begin{bmatrix} L_s & 0 & M_{f\alpha} \\ 0 & L_s & M_{f\beta} \\ M_{f\alpha} & M_{f\beta} & L_f \end{bmatrix} \cdot \frac{d}{dt} \cdot \begin{bmatrix} I_{as} \\ I_{bs} \\ I_{cs} \\ I_f \end{bmatrix} + \begin{bmatrix} e_\alpha \\ e_\beta \\ -e_f \end{bmatrix} . \tag{25}$$

faulty case: $r_f = 7\ \Omega$ and $r_f = 0.5\ \Omega$) when the fault resistance decreases, the three phases currents increase to compensate the negative effects of the short-circuit fault. It can cause a current unbalance in the power supply, and the increase of the absorbed power. We can observe a torque ripple when the faulty case is applied.

Changing the fraction of short-turns means changing the severity of applying fault. From Fig. 4, it is clear that the magnitude of the torque ripple is mainly determined by the severity of the fault. The magnitude of the phase currents and absorbed powerchange proportionally with the severity of the fault and become unbalanced.

It would be very helpful to predict the insulationfailure, breakdown when the fault is not high developed inorder to avoid the machine winding damages [14].

4. Diagnostic of Stator Fault by ESA and EPVA Techniques

Two techniques based on frequency analysis are applied to detect faults in stator, consecutively defined in [15], [16] and [17]. First is ESA, based on the Fast Fourier decomposition of the phase currents winding, the electromagnetic torque and the absorbed power. The second is EPVA, which is based on the frequency analysis of the module of the Park's Vector's of currents as shown below.

4.1. Electric Spectral Analysis (ESA)

We applied this technique on the phase stator currents, the instantaneously absorbed power and the electromagnetic torque. The instantaneous absorbed power is illustrated by the following equation [18]:

$$p(t) = v_{as}(t)i_{as}(t) + v_{bs}(t)i_{bs}(t) + v_{cs}(t)i_{cs}(t). \tag{33}$$

The phase stator currents, the instantaneous absorbed power and electromagnetic torque spectrum analysis results of both healthy and faulty conditions with different values of faulty resistance ($r_f = 100\ \Omega$, $r_f = 7\ \Omega$ and $r_f = 0.5\ \Omega$) of simulation machine are presented in Fig. 5, Fig. 6, and Fig. 7 respectively.

1) Currents Spectral Analysis

The ESA signatures reveal the existence of a spectral component in phase 'a' and 'b', with a small amplitude at the frequency with value three times higher than the supply due the existence of an inter-turn short circuit in the stator winding and its amplitude increase with the increase of severity of faultas seen in Fig. 5(b), Fig. 5(c) and Fig. 5(d), where $r_f = 0.5\ \Omega$ and in Fig. 5(e), where $r_f = 7\ \Omega$, the existence of this harmonic is due to the presence of the third harmonic of the electromotive force presented in Fig. 2(b). We can observe no existence of this harmonic in phase 'c' because the short circuit occurs between phase 'a' and 'b'. Note that at healthy conditions the current does not have this component (third harmonic), as seen in Fig. 5(a).

2) Electromagnetic Torque Spectral Analysis

It is noticeable from Fig. 7, that in case of fault, we notice the appearance of high harmonic at double value of supply frequency, especially if $r_f = 0.5\ \Omega$. The increase of the harmonic amplitude is inversely proportional to the values of fault resistance.

3) Absorbed Power Spectral Analysis

Figure 6 shows the absorbed power spectrum with and without fault. We can observe only a zero frequency component at healthy conditions. In faulty conditions the same analysis as that of the electromagnetic torque is noted. From the comparative analysis of results under healthy and faulty conditions, it is clear that the fault appears in the ESA signaturedue to the presence of harmonic of even rows on the spectrum analysis of electromagnetic torque and absorbed power and by the appearance of the harmonic of odd rows on the spectrum analysis of phase currents. The appearances of these harmonics are directly related to the existence of asymmetries caused by the short-circuit in the stator winding. With the consumption that we have a balanced voltage source, the appearance of harmonics in phase 'a' and 'b' indicates the short-circuit between these two phases.

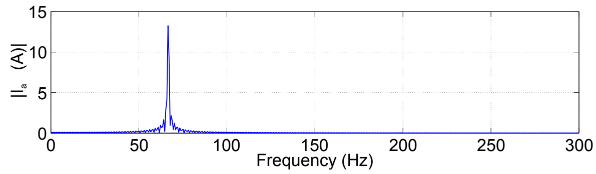

(a) Healthy case for $r_f = 100\ \Omega$.

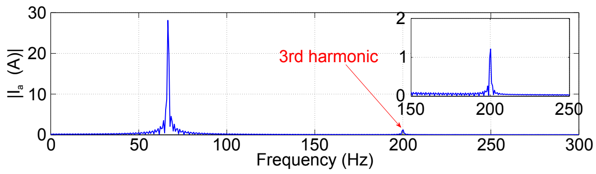

(b) Faulty case for $r_f = 0.5\ \Omega$ (Phase a).

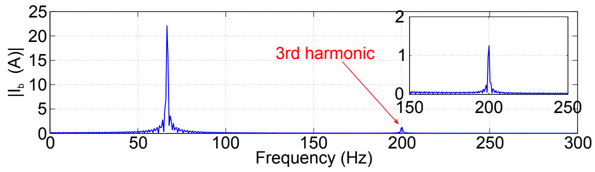

(c) Faulty case for $r_f = 0.5\ \Omega$ (Phase b).

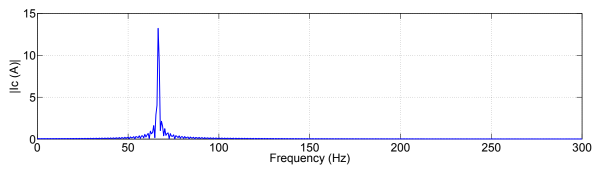

(d) Faulty case for $r_f = 0.5\ \Omega$ (Phase c).

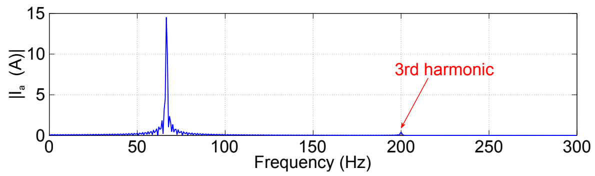

(e) Faulty case for $r_f = 7\ \Omega$

Fig. 5: Spectrum of phase currents.

4.2. Extend Park's Vector Approach (EPVA)

This technique is based on the two equivalent currents in reference frame obtained by Park's transformation [18]:

$$I_d = \sqrt{\frac{2}{3}} \cdot I_{as} - \frac{1}{\sqrt{6}} \cdot I_{bs} - \frac{1}{\sqrt{6}} \cdot I_{cs}, \tag{34}$$

$$I_q = \frac{1}{\sqrt{2}} \cdot I_{bs} - \frac{1}{\sqrt{2}} \cdot I_{cs}, \tag{35}$$

where I_d and I_q are the instantaneous values of electric currents in direct and quadrature axis. Idis always a sine wave and I_q has a cosine wave in healthy conditions. These two components have the same values and their locus is a circle as seen in Fig. 8(a). In case of the inter-turn short circuit, the current becomes unbalanced and it can be expressed as the sum of a positive sequence and a negative sequence component. As a result of this fault, the Concordia's vector locus shape deviates and becomes elliptic as shown in Fig. 8(b).

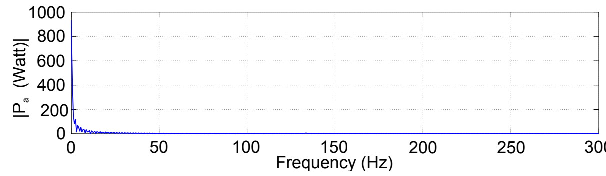

(a) Healthy case for $r_f = 100\ \Omega$.

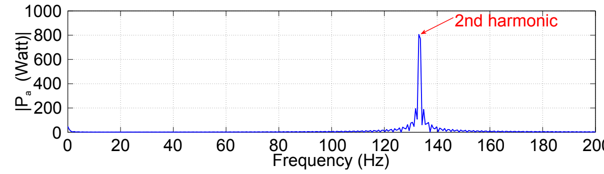

(b) Faulty case for $r_f = 0.5\ \Omega$.

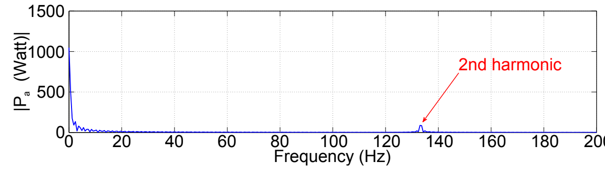

(c) Faulty case for $r_f = 7\ \Omega$.

Fig. 6: Spectrum of absorbed power.

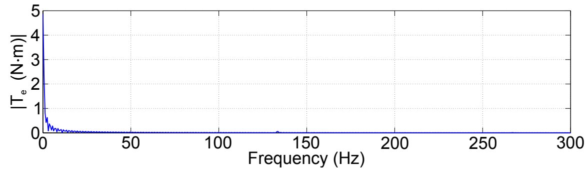

(a) Healthy case for $r_f = 100\ \Omega$.

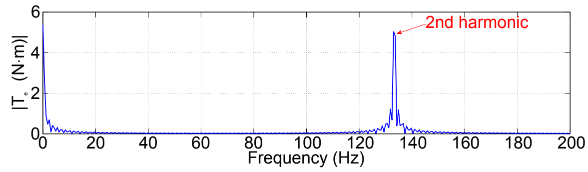

(b) Faulty case for $r_f = 0.5\ \Omega$.

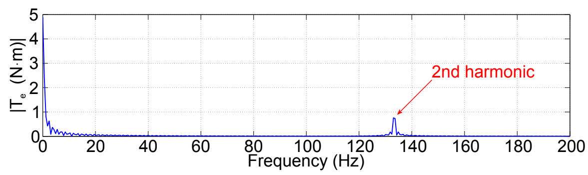

(c) Faulty case for $r_f = 7\ \Omega$.

Fig. 7: Spectrum of electromagnetic torque.

If the motor operates under healthy conditions (i.e. under symmetrical conditions), the three currents form a balanced system and constitute a positive sequence system. Hence, i_d and i_q can be written as below [18]:

$$i_p = \sqrt{i_d^2 + i_q^2}, \tag{36}$$

$$i_d = \frac{\sqrt{6}}{2} \cdot i_{\max} \cdot \sin(\omega t), \tag{37}$$

$$i_q = \frac{\sqrt{6}}{2} \cdot i_{\max} \cdot \sin\left(\omega t - \frac{\pi}{2}\right), \tag{38}$$

where i_{max} is a maximum value of the current positive sequence, ω is the angular supply frequency, and i_p is the Park's equivalent current module. When the system is balanced, the current Park's vector modulus is constant as illustrated in Fig. 9(a). Under faulty condition the currents will contain other components besides the positive sequence component and in this case the Park's Vector modulus will contain a dominant DC and AC level of the motor current supply [15] and their existence is directly related to the asymmetries, as we can see in Fig. 9(b).

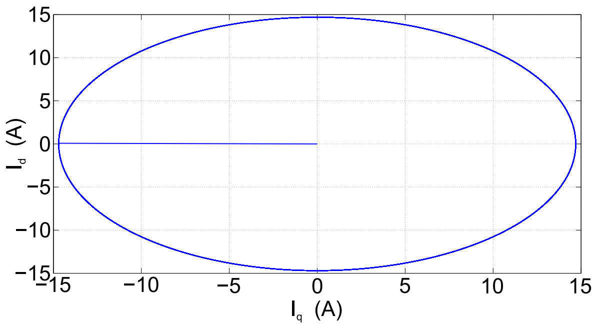

(a) Healthy case.

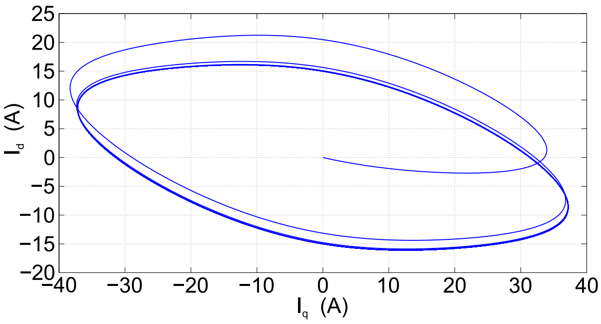

(b) Faulty case.

Fig. 8: Concordia's currents vector locus.

The aim of EPVA technique is to apply the frequency analysis to the Park's vector modulus in order to obtain the EPVA signature when the system is unbalanced. After simulation and analysis, we obtain the results for healthy condition ($r_f = 100\ \Omega$) and faulty conditions ($r_f = 7\ \Omega$ and $r_f = 0.5\ \Omega$) as shown in Fig. 10.

From these results, the EPVA signature reveals the existence of a aspectral component at a frequency of

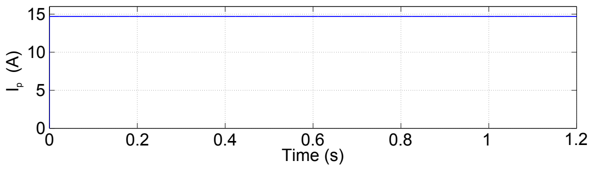

(a) Healthy case.

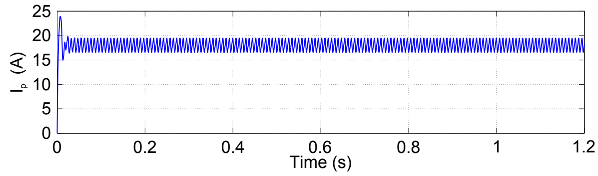

(b) Faulty case.

Fig. 9: Park's vector modulus.

66.67 Hz-twice the fundamental supply frequency and it is so clear from results when the fault resistance decreases (the severity of fault increases) the amplitude of the spectral component makes it a good indicator of the occurred fault.

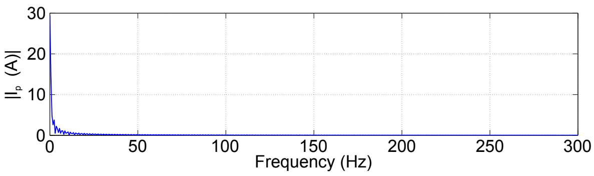

(a) Healthy case for $r_f = 100\ \Omega$.

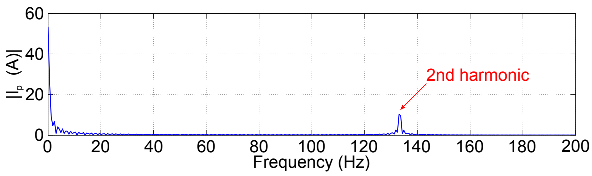

(b) Faulty case for $r_f = 0.5\ \Omega$.

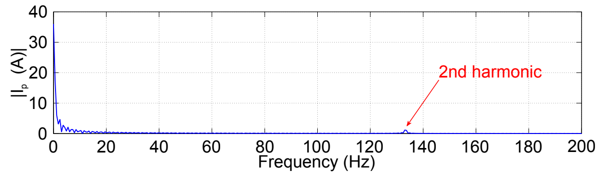

(c) Faulty case for $r_f = 7\ \Omega$.

Fig. 10: Spectrum of Park's vector modulus.

5. Conclusion

This paperproposed a dynamic model for surface mounted PMSM machine under phase-to-phase short-circuit in the stator winding. The real form of back EMF is presented and included in the model. This faulty model is used to study the behavior of the machine under various fault conditions and severity. From the analysis of the simulation results, phase-to-phase short-circuit fault causes high torque ripples and currentunbalance in the system. Higher circulating currents could be generated by the motor winding short-circuit. More importantly, the detection of these kinds of faultsis crucial in the design and development procedure of the motor drive and its diagnosis. Two simple and effective diagnosis method as ESA and EPVA based on frequency analysis are used to analyze and to indicate the presence of the short-circuit fault between two phases in the stator. The appearance of the 2nd and 3rd harmonic indicates the presence of this fault andthe amplitude of the harmonics is proportional to the severity of this fault. The shape of Concordia's currents vector locus is a good indicator of the presence of the fault when its form changes from the circle trajectory to an elliptical one.

References

[1] HADEF, M., M. R. MEKIDECHE and A. O. N'DIAYE. Diagnosis of stator winding short circuit faults in a direct torque controlled interior permanent magnet synchronous motor. In: *IEEE Vehicle Power and Propulsion.* Chicago: IEEE, 2011, pp. 1–8. ISBN 978-61284-247-9. DOI: 10.1109/VPPC.2011.6043166.

[2] VASEGHI, B., B. NAHID-MOBAREKEH, N. TAKORABET and F. MEIBODY-TABAR. Modeling of non-salient PM synchronous machines under stator winding inter-turn fault condition: dynamic model-emfmode. In: *IEEE Vehicle Power and Propulsion Conference.* Arlington: IEEE, 2007, pp. 635–640. ISBN 0-7803-9761-4. DOI: 10.1109/VPPC.2007.4544200.

[3] CAPOLINO, G. A., C. BRUZZESE, R. PUSCA and J. ESTIMA. Trends in fault diagnosis for electrical machines: areview of diagnostic techniques. *IEEE Industrial Electronics Magazine.* 2014, vol. 8, iss. 2, pp. 31–42. ISSN 1932-4529. DOI: 10.1109/MIE.2013.2287651.

[4] PROGOVAC, D., L. Y. WANG and G. YIN. System identification of permanent magnet machines and its applications to inter-turn fault detection. In: *IEEE Transportation Electrification Conference and Expo (ITEC).* Detrit MI: IEEE, 2013, pp. 1–5. ISBN 978-1-4799-0148-7. DOI: 10.1109/ITEC.2013.6573486.

[5] VASEGHI, B., B. NAHID-MOBAREKEH, N. TAKORABET and F. MEIBODY-TABAR. Modeling of IM with stator winding inter-turn fault validated by fem. In: *Electrical Machines Conrerence.* Hammamat: IEEE, 2008, pp. 1–5. ISBN 978-1-4244-1736-0. DOI: 10.1109/ICELMACH.2008.4800130.

[6] GWAN GU, B., J. HYUK CHOI and I. SOUNG JUNG. Inter turn short fault model of PMSMs with series and parallel winding connection. In: *Energy Conversion Congress Conference.* Athlanta: IEEE, 2013, pp. 4388–4395. ISBN 978-1-4799-0336-8. DOI: 10.1109/ECCE.2013.6647287.

[7] TALLAM, R. M., T. G. HABTLER and R. G. HARLEY. Transient model for induction machines with stator winding turn faults. *IEEE Transactions on Industry Applicatin.* 2002, vol. 38, iss. 3, pp. 632–637. ISSN 0093-9994. DOI: 10.1109/TIA.2002.1003411.

[8] ARKAN, M., D. KASTIC-PEROVIC and P. J. NSWORTH. Modeling and simulation of induction motors with inter turn fault for diagnostics. *ELSEVIER Journal of Electric Power System Research (EPSR).* 2005, vol. 75, iss. 1, pp. 57–66. ISSN 0378-7796. DOI: 10.1016/j.epsr.2004.08.015.

[9] DAI, M. and A. SEBASTIAN. Fault analysis of a PM brishless DC motor using finite element method. *IEEE Transaction On Energy Conversion.* 2005, vol. 20, iss. 1, pp. 1–4. ISSN 0885-8969. DOI: 10.1109/TEC.2004.841516.

[10] MOHAMMED, O. A., Z. LIU, S. LIU and N. Y. ABED. Inter turn short circuit fault diagnosis for PM machines using FE based of phase variable model and wavelet analysis. *IEEE Transaction On Magnetic.* 2007, vol. 43, iss. 4, pp. 1729–1732. ISSN 0018-9464. DOI: 10.1109/TMAG.2006.892301.

[11] JOENG, I. I. S. U., B. J. HYON and K. NAM. Dynamic modeling and control for SPMSMs with internal turn short faults. *IEEE Transactionon Power Electronic.* 2013, vol. 28, iss. 7, pp. 3495–3508. ISSN 0885-8993. DOI: 10.1106/TPEL.2012.2222049.

[12] KIM, K.-T., J. HUR, B.-W. KIM and G.-H. KANG. Circulating current calculation using fault modeling of IPM type BLCD motor of inter-turn fault. In: *IEEE Electric machines and Systemsconferenc.* Tokyo: IEEE, 2011, pp. 1–5. ISBN 9781-4577-1043-8. DOI: 10.1109/ICEMS.2011.6073686.

[13] VASEGHI, B., B. NAHID-MOBAREKEH, N. TAKORABET and F. MEIBODY-TABAR. Experimentally validation dynamic fault model for PMSM with stator winding inter-turn fault. In: *Industry Application Society Annual Meeting.* Edmonton: IEEE, 2008, pp. 1–5. ISBN 978-1-4244-2279-1. DOI: 10.1109/08IAS.2008.24.

[14] LAI, C., A. BALAMURALI, V. BOUSABA, K. L. V. IYER and N. KAR. Analysis of stator winding inter-turn short circuit fault in interior and surface mounted permanent magnet traction machines. In: *Transportation Electrification Conference and Expo*. Dearborn: IEEE, 2014, pp. 1–6. ISBN 978-1-4799-2262-8. DOI: 10.1109/ITEC.2014.6861775.

[15] CRUZ, S. M. A. and A. J. M. CARDOSO. Stator winding fault diagnosis in three phasessyncrhronous and asynchronous motor, by the extended Park's vector approach. *IEEE Transaction On Industry Applications*. 2001, vol. 37, iss. 5, pp. 1227–1233. ISSN 1939-9367. DOI: 10.1109/28.952496.

[16] CRUZ, S. M. A. and A. J. M. CARDOSO. Multiple reference frames theory: a new methode for the diagnosis of stator fault inthree phases induction motors, by the extended Park's vector approach. *IEEE Transaction On Energy Conversion*. 2005, vol. 20, iss. 3, pp. 611–619. ISSN 1558-0059. DOI: 10.1109/TEC.2005.847975.

[17] DYONOSIOS, V. S. and D. M. EPAMINONDAS. Induction Motor Stator Fault Diagnosis Technique Using Park Vector Approach and Complex Wavelets. In: *IEEE International Conference on Electric Machinery (ICEM)*. Marseille: IEEE, 2012, pp. 1730–1734. ISBN 978-1-4673-0142-8. DOI: 10.1109/ICEIMach.2012.6350114.

[18] PARRA, A. P., M. C. A. ENCICO, J. O. OCHOA and J. A. P. PENAR. Stator fault diagnosis on squirrel cage induction motor by ESA and EPVA. In: *Power Electronics and Power Quality Applications*. Bogota: IEEE, 2014, pp. 1–6. ISBN 978-1-4799-1007-6. DOI: 10.1109/PEPQA.2013.6614937.

About Authors

Chourouk BOUCHAREB was born in 1975, in Algiers, Algeria. She received an Engineer Diploma in Electrical Engineering in 1999 and an M.Sc. degree in Control engineeringin 2005, both from Electrical Engineering Department of Batna University. Her research interests include the electric machines and their control drives and diagnosis. She is a member at the Laboratory University, named Electromagnetic Induction and Propulsion Systems (LSPIE) of Batna University.

Mohamed-Said NAIT-SAID was bornin 1958, in Batna, Algeria, He received an Engineer Diploma in Electrical Engineering from the National Polytechnic High School of Algiers, Algeria (February 1983), and the M.Sc. degree in Electronics and Control Engineering from Electronics Department at Constantine University in 1992. He received the Ph.D. degree in Electrical Engineering from University of Batna after he accomplished his free scientific research accomplished in Automatic Laboratory of Amiens University in French from 1996 to 1999. Currently he is a full professor at the Electrical Engineering Department of Batna University II and is responsible for the Master course of Control and Diagnosis of the Electrical Systems. From 2000–2005, Dr. Nait-Said was the head of the first created research laboratory in Batna University, named Electromagnetic Induction and Propulsion Systems (LSPIE) of Batna and also in 2006 he has been appointed the head of the scientific committee of the same department. LSPIE has been evaluated by the Algerian ministry of the universities as the best laboratory in Batna University (100 percent satisfied. Dr. Nait-Said has supervised twenty five Masters and ten Ph.D. theses. His research interests include the electric machines and their control drives and diagnosis.

Appendix A - AC Driver Parameters

- $P_N = 5$ kW,
- $P = 4$,
- EMF at 1000 rpm $= 34$ V,
- $I_N = 19$ A.